Long Noncoding RNA AL161729.4 Acts as an miR-760 Sponge to Enhance Colon Adenocarcinoma Proliferation via Activating PI3K/Akt Signaling

Xinhong Liu
Chongqing University of Education
Mengyang Shi
Chongqing University Cancer Hospital
Xue Mi
chongqing university of education
Xin Zhao (zhaoxin@cque.edu.cn)
Chongqing University of Education https://orcid.org/0000-0001-9798-7865

Research Article

Keywords: Colon adenocarcinoma, HYOU1, lncRNA AL161729.4, miR-760, prognosis, survival

Posted Date: October 18th, 2021

DOI: https://doi.org/10.21203/rs.3.rs-964991/v1

Abstract

Background: Colon adenocarcinoma is one of the most common gastrointestinal malignancies with poor prognosis and high mortality. The mRNA-miRNA-lncRNA regulatory network mediated by m6A methylation plays an important role in a variety of cancers including colon adenocarcinoma.

Methods: We integrated and analyzed the gene expression data and clinical information of 473 patients with colon adenocarcinoma and 41 normal samples in The Cancer Genome Atlas database. The luciferase reporter gene experiment is used to detect the targeting effect between gene, miRNA and lncRNA. Real-time PCR and Proliferation assays were performed to detect the biological function of gene, miRNA and lncRNA.

Results: A risk model and Nomogram that could accurately predict the survival time of patients were constructed through informatics analysis. *HYOU1*, AL161729.4, miR-760 are differentially expressed in COAD patients and normal samples and are significantly related to survival, and there is a targeted binding effect between the three.

Conclusions: *HYOU1*-AL161729.4-miR-760 ceRNA regulatory network could regulate the proliferation of SW620 cells through the PI3K/Akt signaling pathway.

Background

Colorectal cancer (CRC) is one of the most common gastrointestinal malignancies with poor prognosis and high mortality; it is also the second leading cause of cancer-related deaths worldwide [1]. More than 2.2 million new cases and 1.1 million deaths are predicted by 2030, and the global burden caused by this is also increasing year by year [2]. Approximately 20%-25% of patients with CRC metastases to distant organs at the time of initial diagnosis [3]. As a key tool for early detection, biomarkers have made great progress in the last few decades and have had a positive impact on the treatment of patients with CRC [4]. Colon adenocarcinoma (COAD) is the most common histological subtype of CRC [5].

N6-methyladenosine (m6A) methylation is one of the most common RNA modifications and plays an important role in various life activities and diseases [6–9]. The m6A modifications mainly include methyltransferase (m6A "writer"), demethylase (m6A "eraser"), and m6A "reader" protein [10, 11]. Recent studies have shown that m6A methylation plays a key role in cancer through various mechanisms and can be used as a marker for early cancer diagnosis [12, 13]. m6A-related lncRNA and miRNA play an important role in a variety of diseases, including cancer [14, 15].

MicroRNA (miRNA) is a small RNA that regulates the expression of complementary messenger RNA. It plays an important role in developmental timing, cell death, cell proliferation, hematopoiesis, and patterning of the nervous system [16]. As RNAs that are longer than 200 nucleotides and do not encode proteins, lncRNAs also play an important role in a variety of life activities and diseases [17]. Recent studies have shown that competing endogenous RNA (ceRNA) networks based on mRNA-miRNA-lncRNA

play an essential role in various diseases, including cancer, and are expected to become new early cancer diagnostic markers and therapeutic targets [18–20]. Taking m6A-related genes and lncRNA as the entry point, constructing and verifying a new mRNA-miRNA-lncRNA regulatory network is urgent for the early diagnosis and treatment of COAD.

In this study, we downloaded and compiled the gene, miRNA, and lncRNA expression data of patients with COAD and their corresponding clinical information from The Cancer Genome Atlas (TCGA) database. A new COAD prognostic risk nomogram and mRNA-miRNA-lncRNA regulatory network were constructed through bioinformatics analysis. The experiment verified that *HYOU1*-AL161729.4-miR-760 passed through the PI3K/Akt signal to mediate the occurrence of COAD.

Methods

Patients and dataset

The gene expression profiles and clinical data of 473 patients with COAD and 41 normal samples were obtained at TCGA. Then, the gene transfer format file with re-annotated gene expression data was used and integrated with clinical information. Gene expression profiles mainly included gene, lncRNA, and miRNA. Clinical information mainly included survival time, survival status, age, sex, and tumor stage. Finally, the expression data and clinical information of m6A-related genes were extracted. It mainly included 8 writer genes (*METTL3*, *METTL14*, *METTL16*, *WTAP*, *VIRMA*, *ZC3H13*, *RBM15*, and *RBM15B*), 13 reader genes (*YTHDC1*, *YTHDC2*, *YTHDF1*, *YTHDF2*, *YTHDF3*, *HNRNPC*, *FMR1*, *LRPPRC*, *HNRNPA2B1*, *IGFBP1*, *IGFBP2*, *IGFBP3*, and *RBMX*), and 2 eraser genes (*FTO* and *ALKBH5*).

Identification of prognosis-related lncRNAs

We first analyzed the co-expression of m6A-related genes and lncRNAs through R packages of “limma” to find the lncRNAs related to m6A and used R packages of “igraph” to draw the co-expression network. Then, we used R packages of “survival” to analyze the survival of m6A-lncRNA and obtained m6A-lncRNA significantly related to the survival of patients with COAD. Finally, the difference in the expression of survival-related m6A-lncRNA was analyzed using the R packages of “limma” in patients with COAD and normal samples.

Construction and verification of the prognostic risk model

We used the least absolute shrinkage and selection operator (LASSO) method to analyze survival-related m6A-lncRNA and selected key lncRNAs to construct a prognostic risk model for patients with COAD. The formula for predicting the risk score of patients using the prognostic risk model was as follows:

$$Risk score = \sum_{i=1}^{n} Coef_i * x_i$$

where *Coef* denotes the coefficient of this gene and *x* denotes the expression level of this gene.

All patients with COAD were randomly divided into training and test groups. In each group, patients with COAD were divided into high-risk and low-risk groups according to the median value of the risk score of the training group. The receiver-operating characteristic (ROC) curve of 1-year, 3-year, and 5-year survival curves, single-factor independent prognostic analysis, multi-factor independent prognosis, and correlation analysis of the survival time and risk score were used to evaluate the constructed prognostic risk model. The area under the curve (AUC) value in the ROC curve was greater than or equal to 0.6, indicating that the model had good prediction accuracy.

Nomogram

We performed Cox proportional-hazards analysis on the gene expression data and information such as age, sex, cancer stage, risk score, and so forth, of patients to construct a nomogram so as to more conveniently and accurately predict the prognostic survival time of patients. At the same time, the ROC curve and calibration curve were drawn to evaluate the accuracy of the analysis.

Functional analysis of the prognostic risk model lncRNA

We used the R packages of “limma” to analyze the correlation between the expression of lncRNA and the risk score of the risk model so as to explore the relationship between the two, and performed survival analysis on these lncRNAs one by one to explore the relationship between these lncRNAs and overall survival. We found the lncRNA that was positively correlated with the risk score and negatively correlated with the overall survival as the follow-up research object (interest lncRNA). Finally, we used the lncATLAS (https://lncatlas.crg.eu/) and lncLocator (http://www.csbio.sjtu.edu.cn/bioinf/lncLocator/) databases to perform subcellular location of the interest lncRNA so as to evaluate whether lncRNA gene knockdown experiments could be performed in the future.

Prediction and functional analysis of lncRNA target miRNA and gene

First, we used The Encyclopedia of RNA Interactomes (ENCORI) (http://starbase.sysu.edu.cn/) online database to predict the target miRNA of the interest lncRNA, and crossed it with the low-expressed miRNA

in patients with COAD to obtain the target miRNA of the interest lncRNA. Second, we predicted the target gene of target miRNA through miRDB (http://mirdb.org/), miRTarBase (http://starbase.sysu.edu.cn/starbase2/index.php), and TargetScan (http://www.targetscan.org/vert_71/) databases. Then, Gene Expression Profiling Interactive Analysis (GEPIA, http://gepia.cancer-pku.cn/) database was used to analyze the expression difference of the target genes so as to find the target genes highly expressed in patients with COAD. Finally, an lncRNA-miRNA-gene ceRNA regulatory network significantly related to the survival of patients was constructed based on the principle of base complementary pairing.

Gene expression vector construction

The base sequence of the CD region of *HYOU1* [full length 3000 base pairs (bp)] was chemically synthesized using the whole gene synthesis technology, and then constructed into the pIRES2-EGFP vector (Tsingke, Beijing, China) to obtain the overexpression vector of *HYOU1*. The binding site of miR-760 in the 3'-untranslated region (UTR) of *HYOU1* was found, 500-bp upstream and downstream of the binding site were chemically synthesized, and the site was constructed into the pSi-Check2 vector to construct the *HYOU1* wild-type 3'-UTR vector. In the same way, a wild-type vector of AL161729.4 (length 476 bp) was constructed. Using the point mutation method, *HYOU1* mut-type 3'-UTR vector and AL161729.4 mut-type vector were constructed. *HYOU1* siRNA1#, *HYOU1* siRNA2#, AL161729.4 siRNA1#, AL161729.4 siRNA2#, siRNA negative control, miR-760 mimics, mimics negative control, miR-760 inhibitors, and inhibitor negative control were chemically synthesized (Gene Pharma, Shanghai, China). The sequence is shown in Table 1.

Cell culture and luciferase reporter gene experiment

HT29 and SW620 cells were purchased from the National Collection of Authenticated Cell Cultures (Shanghai, China) and cultured in a 37°C cell incubator containing 5% CO_2. The medium of HT29 cells was McCoy's 5A medium (HyClone,Waltham, MA, USA), and the medium of SW620 was Leibovitz's L-15 (HyClone). Media were supplemented with 10% fetal bovine serum (Invitrogen, Carlsbad, CA, USA), 100 U/ml penicillin, and 100 ug/ml streptomycin (Invitrogen). Lipofectamine 3000 transfection reagent (Invitrogen) was used to transfect the corresponding gene expression vector and oligonucleotides into the cells, the cell culture was continued for 48 h, and the cells were then lysed. The Dual-Luciferase Reporter Assay System (Promega, WI, USA) was used to detect the fluorescence level so as to detect the targeted binding between lncRNA-miRNA-gene.

RNA extraction and quantitative polymerase chain reaction

The gene expression vector and oligonucleotides were transfected into the HT29 and SW620 cells and cultured for 48 h. TRIzol reagent (Invitrogen) was used to lyse the cells and extract total RNA. Then, a

RevertAid First-Strand cDNA Synthesis Kit (Thermo Fisher Scientific, MA, USA) was used for reverse transcription to obtain cDNA. Finally, SYBR Green Polymerase Chain Reaction (PCR) Master Mix (Thermo Fisher Scientific) was used to perform fluorescence quantitative PCR, and the relative expression of genes was determined by the $2^{-\Delta\Delta Ct}$ method. All primer sequences are listed in Table 2.

Cell proliferation assay

The HT29 and SW620 cells were seeded into 96-well plates at a density of 2×10^4 cells per well, and the culture was continued for 24 h. Then, we changed the fresh medium and transfected the gene expression vector and oligonucleotides into cells. These cells were mixed with 10 μL of MTT staining solution and incubated for 4 h on days 1, 3, 5, and 7 after transfection. Then, the MTT cell proliferation assay (Solarbio, Beijing, China) was used to detect cell proliferation. The absorbance was measured at 490 nm. All experiments were performed in triplicate.

Statistical analysis

In the co-expression analysis of m6A-related genes and lncRNA, Pearson correlation coefficient ≥0.4 and P <0.001 are the criteria for judging whether they were related. In the analysis of survival difference and expression difference, P <0.001 indicated a significant difference. All experiments were performed independently at least three times with similar results, and representative experiments were shown. P <0.05 was considered statistically significant (NS > 0.05; $^{*}P$ < 0.05; $^{**}P$ < 0.01; $^{***}P$ < 0.001).

Results

Prognosis-related lncRNA

The co-expression analysis confirmed that 1616 lncRNAs had a co-expression relationship with m6A-related genes (Fig. 1A). Survival analysis results showed that ATP2B1-AS1, NSMCE1-DT, AC003101.2, LINC02657, AL161729.4, ZKSCAN2-DT, AP006621.2, AC156455.1, NIFK-AS1, AC008760.1, and AC245041.1 were significantly related to the survival of patients with COAD (Fig. 1B). The results of expression analysis showed that the expression of these 13 lncRNAs significantly related to survival had significant differences between patients with COAD and normal samples (Fig. 1C).

Construction and verification of the prognostic risk model

LASSO regression analysis further confirmed that AC003101.2, LINC02657, L161729.4, AP006621.2, AC156455.1, ZKSCAN2-DT, and AC245041.1 were key lncRNAs, which could be used to construct a prognostic risk model (Fig. 2A and 2B). The formula for calculating the risk score of patients with COAD was as follows:

Risk score = (0.7734 × Exp AC003101.2) + (0.5589 × Exp LINC02657) + (0.0020 × ExpAL161729.4) + (0.0678 × ExpAP006621.2) + (0.0914 × Exp AC156455.1) + (0.4037 × Exp ZKSCAN2-DT) + (0.1692 × Exp AC245041.1) (Fig. 2C).

A significant difference in survival was found between the high-risk and the low-risk groups in the training group; the survival rate in the low-risk group was significantly higher than that in the high-risk group (Fig. 2D). The AUC value of the 1-year, 3-year, and 5-year survival curves was 0.766, 0.785, and 0.726, respectively, which showed that the survival curve was credible (Fig. 2E). The calibration curve of the survival curve further verified its credibility (Fig. 2F). The trend in the test group was the same as that in the train group (Fig. 2G-2I). The survival status results showed that the higher the risk score of patients, the greater the number of deaths (Fig. 2M and 2N). The results of correlation analysis showed that the overall survival rate of patients was negatively correlated with the risk score, although the statistical difference was not significant (Fig. 2O and 2P). Single-factor independent prognostic analysis and multivariate independent prognostic analysis showed that whether in the train group or in the test group, the risk score could be used as a key factor to predict the prognostic survival rate of COAD (Fig. 2Q-2T).

Nomogram

By integrating factors such as age, sex, cancer stage, and risk score of patients, we constructed a nomogram that could predict the 1-year, 3-year, and 5-year survival rates of patients (Fig. 3A). For each patient, the overall score could be calculated according to the scores of the four factors of age, sex, cancer stage, and risk score. Finally, the survival rate could be obtained according to the score and the horizontal axis of the survival rate. The AUC values of the ROC curve of 1 year, 3 years, and 5 years were all greater than 0.8, indicating that the constructed nomogram had good prediction accuracy. The calibration curve of the ROC curve also illustrated this point.

Functional analysis of the prognostic risk model lncRNA

The analysis between the risk score and the expression of lncRNA showed a positive correlation between AC003101.2, LINC02657, AL161729.4, AP006621.2, AC156455.1, ZKSCAN2-DT, AC245041.1, and the risk score. The higher the level of expression, the higher the risk score. This implied that these lncRNAs might be involved in the occurrence and development of COAD (Fig. 4A-4G). The results of survival analysis showed that L161729.4, AP006621.2, and AC156455.1 were significantly related to the survival of patients, and the higher the expression of lncRNA, the lower the survival rate of COAD (Fig. 4H-4N). The full length of AL161729.4 was only 476 bp with only one transcript; therefore, we determined it as the target of follow-up research. The results of subcellular localization showed that AL161729.4 mainly existed in the cytoplasm in GM12878, MCF7, and other cells (Fig. 4O). The subcellular localization results of the prediction model showed that about 40% of lncRNA AL161729.4 was located in the cytoplasm (Fig. 4P). The results of subcellular localization showed that the knockdown vector designed and

constructed for lncRNA could decrease the content of AL161729.4 *in vivo*. Then, the function of lncRNA AL161729.4 was examined.

Construction of ceRNA network

ENCORI online database results showed that the target miRNA of lncRNA AL161729.4 included miR-498-5p, miR-4291, miR-4762-3p, miR-6759-5p, miR-181b-3p, miR-181b-2-3p, miR-4306, miR-711, miR-555, miR-6776-5p, miR-100-3p, miR-3684, miR-6507-5p, miR-4420, miR-182-5p, miR-4644, miR-185-5p, miR-631, miR-3661, miR-3123, miR-760, miR-299-3p, miR-10524-5p, miR-6529-5p, miR-1909-3p, miR-451b, miR-8065, miR-5196-5p, miR-4747-5p, miR-12131, miR-4441, miR-6873-5p, miR-6722-3p, and miR-609. The results of miRNA difference analysis showed that 180 highly expressed miRNAs existed in normal samples, including miR-760, compared with patients with COAD (Fig. 5A). The survival analysis of miR-760 showed that the higher the expression of miR-760, the higher the survival rate of patients. This indicated that miR-760 might play a positive regulatory role in the development of COAD (Fig. 5B).

The miRNA target gene prediction results showed 24 miR-760 target genes predicted by the three databases miRDB, miRTarBase, and TargetScan: *HM13*, *ORAI2*, *AKAP12*, *GOLGA7*, *HIST1H2AE*, *HIST2H2BE*, *HYOU1*, *KHNYN*, *MAGED1*, *SRRM1*, *PUM1*, *GDE1*, *RIC8A*, *KIAA1191*, *PPIP5K1*, *NFATC2IP*, *ANP32B*, *ANKFY1*, *STEAP3*, *HMGA2*, *TRAPPC10*, *PDXK*, *FOXJ2*, and *TOMM40L* (Fig. 5C). The gene expression differential analysis showed that *STEAP3*, *PDXK*, *HYOU1*, and *HM13* were highly expressed in patients, while *HMGA2*, *AKAP12*, and *ANKFY1* were highly expressed in normal samples (Fig. 5D-5J). The ceRNA network of AL161729.4-miR-760-HYOU1 was constructed based on the principle of base complementary pairing (Fig. 5K).

Verification of ceRNA network

When miR-760 mimics were transfected into HT29 and SW620 cells, the fluorescence luminescence of wild-type expression vectors of *HYOU1* and AL161729.4 reduced (Fig. 6A-6D). When miR-760 inhibitors were transfected into HT29 and SW620 cells, the fluorescence of wild-type expression vectors of *HYOU1* and AL161729.4 increased (Fig. 6E-6H). The overexpression and inhibition results of miR-760 indicated that miR-760 could indeed target binding to AL161729.4 and *HYOU1*, and the AL161729.4-miR-760-*HYOU1* ceRNA network existed.

AL161729.4-miR-760-*HYOU1* was involved in regulating the PI3K/Akt signaling pathway

In the detection of the knockdown efficiency of the knockdown vector, it was found that the knockdown effect of AL161729.4 siRNA 1# was significantly better than that of siRNA 2# (Fig. 7A), and the knockdown effect of *HYOU1* siRNA 2# was better than that of siRNA 1# (Fig. 7B). In subsequent studies,

the knockdown vectors with better effects were used for experiments. MiR-760 mimics could significantly reduce the mRNA levels of AL161729.4, *HYOU1*, *PI3K*, and *Akt* (Fig. 7C), and miR-760 inhibitors could increase their mRNA levels (Fig. 7D).

AL161729.4-miR-760-HYOU1 was involved in cancer cell proliferation

The overexpression of AL161729.4 could promote the proliferation of SW620 (Fig. 8A), while the knockdown of AL161729.4 could inhibit the proliferation of SW620 (Fig. 8B). MiR-760 mimics could inhibit the proliferation of SW620 (Fig. 8C), while miR-760 inhibitors could promote the proliferation of SW620 (Fig. 8D). The overexpression of *HYOU1* could promote the proliferation of SW620 (Fig. 8E), while the knockdown of *HYOU1* could inhibit the proliferation of SW620 (Fig. 8F). These findings proved that AL161729.4-miR-760-*HYOU1* directly participated in the regulation of SW620 cell proliferation.

Discussion

The poor prognosis caused by the inability of the early diagnosis of COAD has always been a medical challenge. Hence, more comprehensive and accurate diagnostic markers and therapeutic targets are urgently needed [21–23]. m6A modifications regulate the occurrence and development of a variety of cancers through lncRNAs and miRNAs [24–27]. For example, m6A writer-METTL14 suppresses the proliferation and metastasis of colorectal cancer by downregulating oncogenic long noncoding RNA XIST [28]. m6A writers-METTL3 and eraser-ALKBH5 promoted the invasion and metastasis of cancer cells [29, 30]. However, the current research on the occurrence and regulation of COAD mediated by the mRNA-miRNA-lncRNA regulatory network based on m6A modifications has not been in depth. In this study, we used bioinformatics methods to construct a new mRNA-miRNA-lncRNA regulatory network based on m6A modifications, and experimentally verified how it regulated the occurrence and development of COAD.

Through single-factor Cox regression analysis, we determined that 11 m6A-related lncRNAs were significantly related to the prognosis of COAD, and further used LASSO regression analysis to find seven most critical lncRNAs. The prognostic risk model and the nomogram constructed based on this were also verified by survival analysis, ROC curve, and calibration curve. We constructed the *HYOU1*-AL161729.4-miR-760 regulatory network through expression difference analysis, survival analysis, and target combination prediction. *HYOU1*, AL161729.4, and miR-760 were all significantly related to the survival of COAD or a significant difference in expression existed between patients with COAD and normal samples.

The protein encoded by *HYOU1* belongs to the heat shock protein 70 family. It is found to be highly expressed in a variety of tumors and is associated with tumor aggressiveness and poor prognosis [31–35]. AL161729.4 has 476 nucleotides [36], which is suitable for constructing an overexpression vector. It is mainly located in the cytoplasm [37, 38], and hence it is also convenient for knockdown vectors to knock it down. Currently, no report exists on the function of AL161729.4. It is a brand new lncRNA with

unknown function. Studies have shown that microRNA-760 can inhibit the proliferation and invasion of colorectal cancer cells through the PTEN/Akt signaling pathway [39]. Studies have shown that *HYOU1* promotes cell growth and metastasis by activating PI3K/Akt signals and leads to poor prognosis [40]. Combined with the targeting relationship between *HYOU1*-AL161729.4-miR-760, we predicted that the *HYOU1*-AL161729.4-miR-760 regulatory network will regulate the occurrence of COAD through the PI3K/Akt signaling pathway.

We constructed overexpression vectors and knockdown vectors of *HYOU1*, AL161729.4, and miR-760 through genetic engineering and chemical synthesis. The experimental results of the luciferase reporter gene proved a targeted binding effect among the three. The results of qPCR experiments further confirmed the reliability of the *HYOU1*-AL161729.4-miR-760 regulatory network and its relationship with the PI3K/Akt signaling pathway. Finally, the cell proliferation experiment confirmed that the *HYOU1*-AL161729.4-miR-760 regulatory network was involved in the proliferation regulation of SW620 cells.

Our study involved bioinformatics analysis. We constructed a COAD prognostic risk model and nomogram based on m6A-related lncRNA and experimentally verified the latest mRNA-miRNA-lncRNA regulatory network. However, the findings were still inadequate. First, because of the research conditions, we only explored the effect of the *HYOU1*-AL161729.4-miR-760 regulatory network on the proliferation of SW620 cells, and did not conduct research on invasion and infiltration. In addition, the effect of the *HYOU1*-AL161729.4-miR-760 regulatory network on the occurrence and development of COAD has not been investigated *in vivo*.

Conclusions

In this study, we integrated the COAD gene, lncRNAs, miRNAs, and clinical information to construct a risk model and nomogram that could accurately predict the prognosis of patients with COAD. The *HYOU1*-AL161729.4-miR-760 regulatory network was constructed, and experiments proved that it regulated the proliferation of SW620 cells by mediating the PI3K/Akt signaling pathway. Our study provided new biomarkers for the early diagnosis of COAD and also a new target for further in-depth study of the occurrence and development of COAD.

Declarations

Acknowledgements

Not applicable.

Authors’ contributions

XHL analyzed and interpreted the patient data and was a major contributor in writing the manuscript. MYS performed in vitro studies. XM was responsible for the statistical analysis. XZ oversaw the research

and reviewed the final manuscript. All authors read and approved the final manuscript.

Funding

This research was funded by the Chongqing University Innovation Research Group Project (CXQTP20033) and the Science and Technology Project of Chongqing Education Commission (KJQN202001604)

Availability of data and materials

The datasets generated and/or analysed during the current study are available from the corresponding author on request

Ethics approval and consent to participate

The study follows the principles of the Declaration of Helsinki.

Consent for publication

We would like to declare on behalf of my co-authors that the work described was original research that has not been published previously, and not under consideration for publication elsewhere, in whole or in part. No confict of interest exits in the submission of this manuscript, and manuscript is approved by all authors for publication.

Competing interests

The authors declare that they have no competing financial interests.

References

1. Siegel RL, Miller KD, Jemal A. Cancer statistics, 2019. CA Cancer J Clin. 2019;69(1):7–34.
2. Arnold M, Sierra MS, Laversanne M, Soerjomataram I, Jemal A, Bray F. Global patterns and trends in colorectal cancer incidence and mortality. Gut. 2017;66(4):683–91.
3. Kim K, Kim YW, Shim H, Kim BR, Kwon HY. Differences in clinical features and oncologic outcomes between metastatic right and left colon cancer. J BUON. 2018;23(7):11–8.
4. Ogunwobi OO, Mahmood F, Akingboye A. Biomarkers in Colorectal Cancer: Current Research and Future Prospects. Int J Mol Sci. 2020;21(15):5311.
5. Wang H, Liu J, Li J, Zang D, Wang X, Chen Y, Gu T, Su W, Song N. Identification of gene modules and hub genes in colon adenocarcinoma associated with pathological stage based on WGCNA analysis.

Cancer Genet. 2020;242:1–7.

6. Roundtree IA, Evans ME, Pan T, He C. Dynamic RNA Modifications in Gene Expression Regulation. Cell. 2017;169(7):1187–200.
7. Lin S, Choe J, Du P, Triboulet R, Gregory RI. The m(6)A Methyltransferase METTL3 Promotes Translation in Human Cancer Cells. Mol Cell. 2016;62(3):335–45.
8. Yang C, Hu Y, Zhou B, Bao Y, Li Z, Gong C, Yang H, Wang S, Xiao Y. The role of m6A modification in physiology and disease. Cell Death Dis. 2020;11(11):960.
9. Wang X, Zhao BS, Roundtree IA, Lu Z, Han D, Ma H, Weng X, Chen K, Shi H, He C. N(6)-methyladenosine Modulates Messenger RNA Translation Efficiency. Cell. 2015;161(6):1388–99.
10. Wang X, Lu Z, Gomez A, Hon GC, Yue Y, Han D, Fu Y, Parisien M, Dai Q, Jia G, et al. N6-methyladenosine-dependent regulation of messenger RNA stability. Nature. 2014;505(7481):117–20.
11. Liu T, Wei Q, Jin J, Luo Q, Liu Y, Yang Y, Cheng C, Li L, Pi J, Si Y, et al. The m6A reader YTHDF1 promotes ovarian cancer progression via augmenting EIF3C translation. Nucleic Acids Res. 2020;48(7):3816–31.
12. Barbieri I, Tzelepis K, Pandolfini L, Shi J, Millán-Zambrano G, Robson SC, Aspris D, Migliori V, Bannister AJ, Han N, et al. Promoter-bound METTL3 maintains myeloid leukaemia by m6A-dependent translation control. Nature. 2017;552(7683):126–31.
13. Müller S, Glaß M, Singh AK, Haase J, Bley N, Fuchs T, Lederer M, Dahl A, Huang H, Chen J, et al. IGF2BP1 promotes SRF-dependent transcription in cancer in a m6A- and miRNA-dependent manner. Nucleic Acids Res. 2019;47(1):375–90.
14. Yang D, Qiao J, Wang G, Lan Y, Li G, Guo X, Xi J, Ye D, Zhu S, Chen W, et al. N6-Methyladenosine modification of lincRNA 1281 is critically required for mESC differentiation potential. Nucleic Acids Res. 2018;46(8):3906–20.
15. Zepecki JP, Karambizi D, Fajardo JE, Snyder KM, Guetta-Terrier C, Tang OY, Chen JS, Sarkar A, Fiser A, Toms SA, Tapinos N. miRNA-mediated loss of m6A increases nascent translation in glioblastoma. PLoS Genet. 2021;17(3):e1009086.
16. Ambros V. The functions of animal microRNAs. Nature. 2004;431(7006):350–5.
17. Kopp F, Mendell JT. Functional Classification and Experimental Dissection of Long Noncoding RNAs. Cell. 2018;172(3):393–407.
18. Qi X, Zhang DH, Wu N, Xiao JH, Wang X, Ma W. ceRNA in cancer: possible functions and clinical implications. J Med Genet. 2015;52(10):710–8.
19. Zhang M, Zhao K, Xu X, Yang Y, Yan S, Wei P, Liu H, Xu J, Xiao F, Zhou H, et al. A peptide encoded by circular form of LINC-PINT suppresses oncogenic transcriptional elongation in glioblastoma. Nat Commun. 2018;9(1):4475.
20. Samir N, Matboli M, El-Tayeb H, El-Tawdi A, Hassan MK, Waly A, El-Akkad HAE, Ramadan MG, Al-Belkini TN, El-Khamisy S, El-Asmar F. Competing endogenous RNA network crosstalk reveals novel molecular markers in colorectal cancer. J Cell Biochem. 2018;119(8):6869–81.

21. Sveen A, Kopetz S, Lothe RA. Biomarker-guided therapy for colorectal cancer: strength in complexity. Nat Rev Clin Oncol. 2020;17(1):11–32.
22. Brody H. Colorectal cancer. Nature. 2015;521(7551):1.
23. Zamani M, Hosseini SV, Mokarram P. Epigenetic biomarkers in colorectal cancer: premises and prospects. Biomarkers. 2018;23(2):105–14.
24. Fazi F, Fatica A. Interplay between N6-methyladenosine (m6A) and non-coding RNAs in cell development and cancer. Front Cell Dev Biol. 2019;7:116.
25. Peng L, Yuan X, Jiang B, Tang Z, Li GC. LncRNAs: key players and novel insights into cervical cancer. Tumour Biol. 2016;37(3):2779–88.
26. Yi YC, Chen XY, Zhang J, Zhu JS. Novel insights into the interplay between m6A modification and noncoding RNAs in cancer. Mol Cancer. 2020;19(1):121.
27. Qin Y, Li L, Luo E, Hou J, Yan G, Wang D, Qiao Y, Tang C. Role of m6A RNA methylation in cardiovascular disease (Review). Int J Mol Med. 2020;46(6):1958–72.
28. Yang X, Zhang S, He C, Xue P, Zhang L, He Z, Zang L, Feng B, Sun J, Zheng M. METTL14 suppresses proliferation and metastasis of colorectal cancer by down-regulating oncogenic long non-coding RNA XIST. Mol Cancer. 2020;19(1):46.
29. Xue L, Li J, Lin Y, Liu D, Yang Q, Jian J, Peng J. m6 A transferase METTL3-induced lncRNA ABHD11-AS1 promotes the Warburg effect of non-small-cell lung cancer. J Cell Physiol. 2021;236(4):2649–58.
30. Zhang J, Guo S, Piao HY, Wang Y, Wu Y, Meng XY, Yang D, Zheng ZC, Zhao Y. ALKBH5 promotes invasion and metastasis of gastric cancer by decreasing methylation of the lncRNA NEAT1. J Physiol Biochem. 2019;75(3):379–89.
31. Wang JM, Jiang JY, Zhang DL, Du X, Wu T, Du ZX. HYOU1 facilitates proliferation, invasion and glycolysis of papillary thyroid cancer via stabilizing LDHB mRNA. J Cell Mol Med. 2021;25(10):4814–25.
32. Zong ZH, Du ZX, Zhang HY, Li C, An MX, Li S, Yao HB, Wang HQ. nvolvement of Nrf2 in proteasome inhibition-mediated induction of ORP150 in thyroid cancer cells. Oncotarget. 2016;7(3):3416–26.
33. Lee M, Song Y, Choi I, Lee SY, Kim S, Kim SH, Kim J, Seo HR. Expression of HYOU1 via reciprocal crosstalk between NSCLC cells and HUVECs control cancer progression and chemoresistance in tumor spheroids. Mol Cells. 2021;44(1):50–62.
34. Zhou Y, Liao Q, Li X, Wang H, Wei F, Chen J, Yang J, Zeng Z, Guo X, Chen P, et al. HYOU1, regulated by LPLUNC1, is up-regulated in nasopharyngeal carcinoma and associated with poor prognosis. J Cancer. 2016;7(4):367–76.
35. Stojadinovic A, Hooke JA, Shriver CD, Nissan A, Kovatich AJ, Kao TC, Ponniah S, Peoples GE, Moroni M. HYOU1/Orp150 expression in breast cancer. Med Sci Monit. 2007;13(11):BR231–9.
36. Volders PJ, Anckaert J, Verheggen K, Nuytens J, Martens L, Mestdagh P, Vandesompele J. LNCipedia 5: towards a reference set of human long non-coding RNAs. Nucleic Acids Res. 2019;47(D1):D135–9.

37. Mas-Ponte D, Carlevaro-Fita J, Palumbo E, Hermoso Pulido T, Guigo R, Johnson R. LncATLAS database for subcellular localization of long noncoding RNAs. RNA. 2017;23(7):1080–7.
38. Cao Z, Pan X, Yang Y, Huang Y, Shen HB. The lncLocator: a subcellular localization predictor for long non-coding RNAs based on a stacked ensemble classifier. Bioinformatics. 2018;34(13):2185–94.
39. Li X, Ding Y, Liu N, Sun Q, Zhang J. MicroRNA–760 inhibits cell proliferation and invasion of colorectal cancer by targeting the SP1–mediated PTEN/AKT signalling pathway. Mol Med Rep. 2017;16(6):9692–700.
40. Li X, Zhang NX, Ye HY, Song PP, Chang W, Chen L, Wang Z, Zhang L, Wang NN. HYOU1 promotes cell growth and metastasis via activating PI3K/AKT signaling in epithelial ovarian cancer and predicts poor prognosis. Eur Rev Med Pharmacol Sci. 2019;23(10):4126–35.

Tables

Table 1: Sequences of the primers used for this experiment.

Name	Sequences (5'–3')
miR-760 mimics	CGGCUCUGGGUCUGUGGGGA
	CCCACAGACCCAGAGCCGUU
miR-760 inhibitors	UCCCCACAGACCCAGAGCCG
AL161729.4 siRNA1#	GCCUCUCCCUGUCUAAUAUTT
	AUAUUAGACAGGGAGAGGCTT
AL161729.4 siRNA2#	GCUGGAGCAACAAAUUUAUTT
	AUAAAUUUGUUGCUCCAGCTT
HYOU1 siRNA1#	GGGCAUGGUUCUAAUUAUTT
	AUAAUUGAGAACCAUGCCCTT
HYOU1 siRNA2#	GCUCAGCAAAGCCUUUAAATT
	UUAAAGGCUUUGCUGAGCTT
siRNA NC	UUCUUCGAACGUGUCACGUTT
mimics NC	UUCUUCGAACGUGUCACGUTT
inhibitors NC	CAGUACUUUUGUGUAGUACAA

Table 2: Sequences of the primers used for this experiment.

Name	Sequences (5'–3')
AL161729.4 F	5'-ACTCCAGGTCTAAATACTAG-3'
AL161729.4 R	5'-GTTCAAAGTCTGGGTGTTGT-3'
HYOU1 F	5'-CTTCCACATCAACTACGGCG-3'
HYOU1 R	5'-CTCTTCTGCGCTGTCCTCTA-3'
PI3K F	5’-GGGGATGATTTACGGCAAGATA-3’
PI3K R	5’-CACCACCTCAATAAGTCCCACA-3’
Akt F	5’-GCAGCACGTGTACGAGAAGA-3’
Akt R	5’-GGTGTCAGTCTCCGACGTG-3’
β-actin F	5'-TCACCCACACTGTGCCCCATCTACGA-3'
β-actin R	5'-TCGGTGAGGATCTTCATGAGGTA-3'

Figures

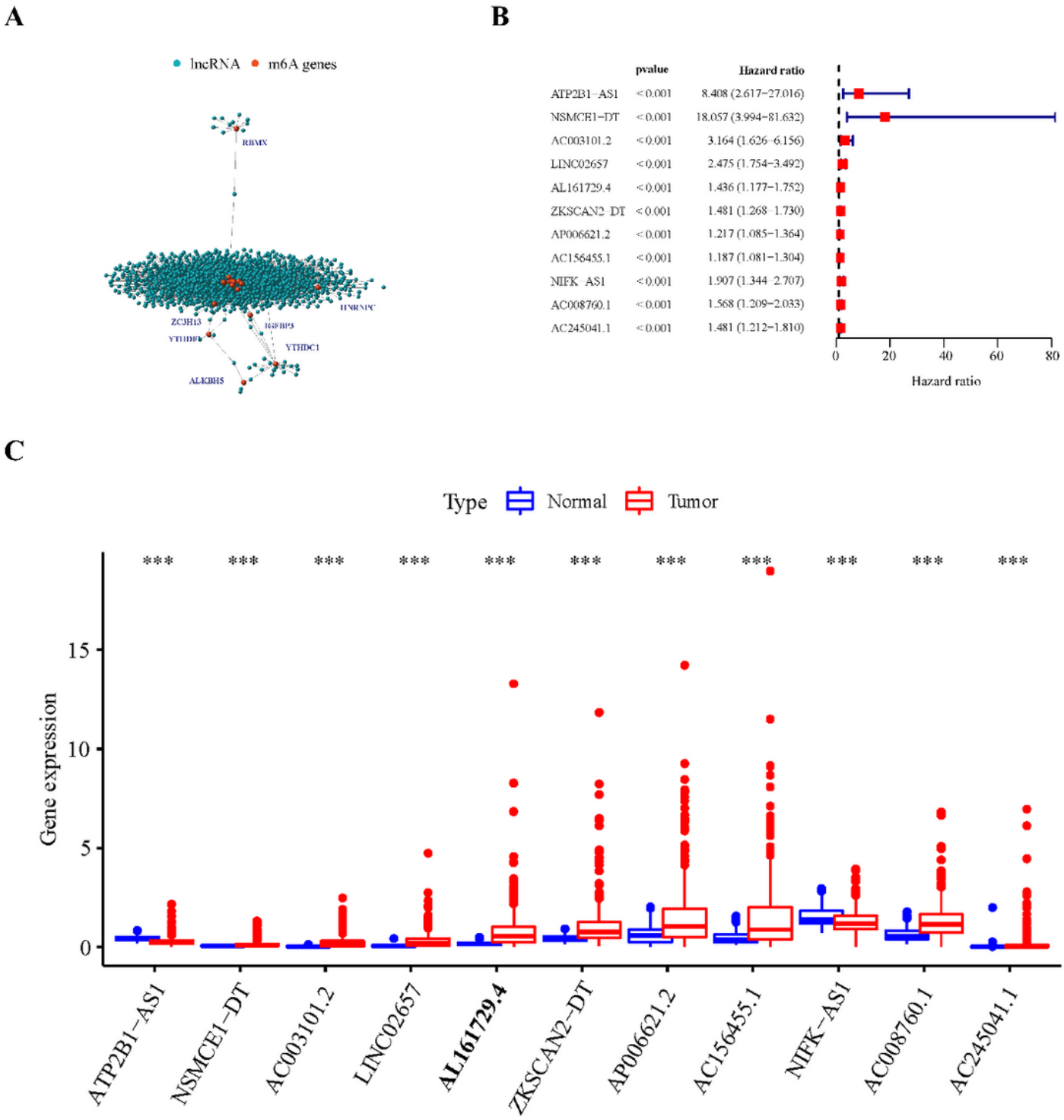

Figure 1

Prognosis-related lncRNA. (A) 1616 lncRNAs and m6A gene co-expression network. (B) A forest plot of 11 lncRNAs significantly correlated with the survival of patients with COAD. (C) Significant differences were found in the expression of 11 lncRNAs between patients with COAD and normal samples.

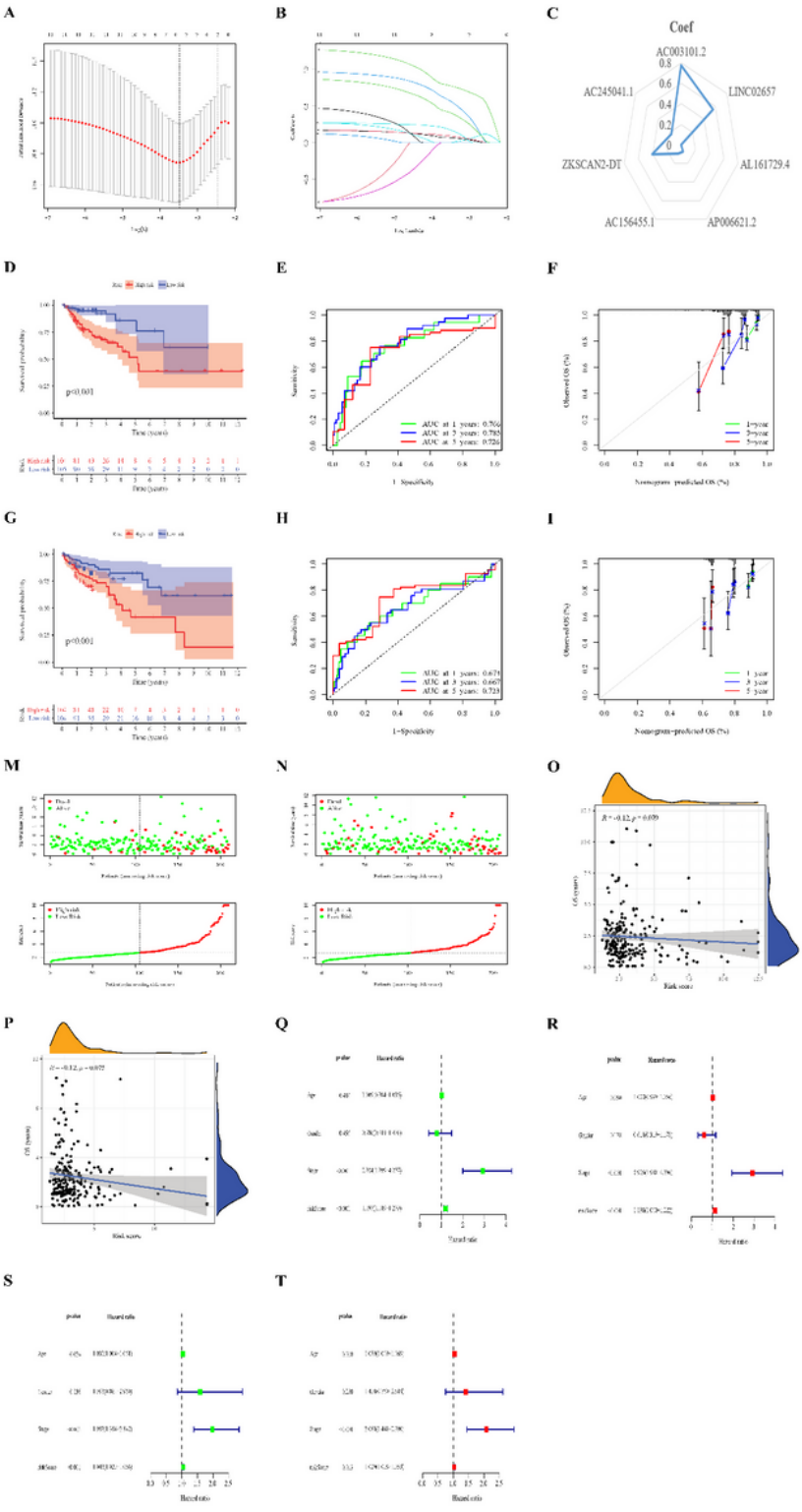

Figure 2

Construction and verification of the prognostic risk model. (A and B) The LASSO model identified the seven key lncRNAs. (C) Regression coefficients of seven key lncRNAs. (D) A significant difference in survival was found between the high-risk and low-risk groups in the train group. (E) ROC curve in the train group for 1 year, 3 years, and 5 years. (F) Calibration curve of the ROC curve in the train group for 1 year, 3 years, and 5 years. (G) A significant difference in survival was observed between the high-risk and low-

risk groups in the test group. (H) ROC curve in the test group for 1 year, 3 years, and 5 years. (I) Calibration curve of the ROC curve in the test group for 1 year, 3 years, and 5 years. (M and N) Survival status and risk score of patients with COAD in the train and test groups. (O and P) Risk score of patients in the train and test groups was negatively correlated with overall survival. (Q and R) Independent prognostic analysis of a single factor and multiple factors in the train group. (S and T) Independent prognostic analysis of a single factor and multiple factors in the test group.

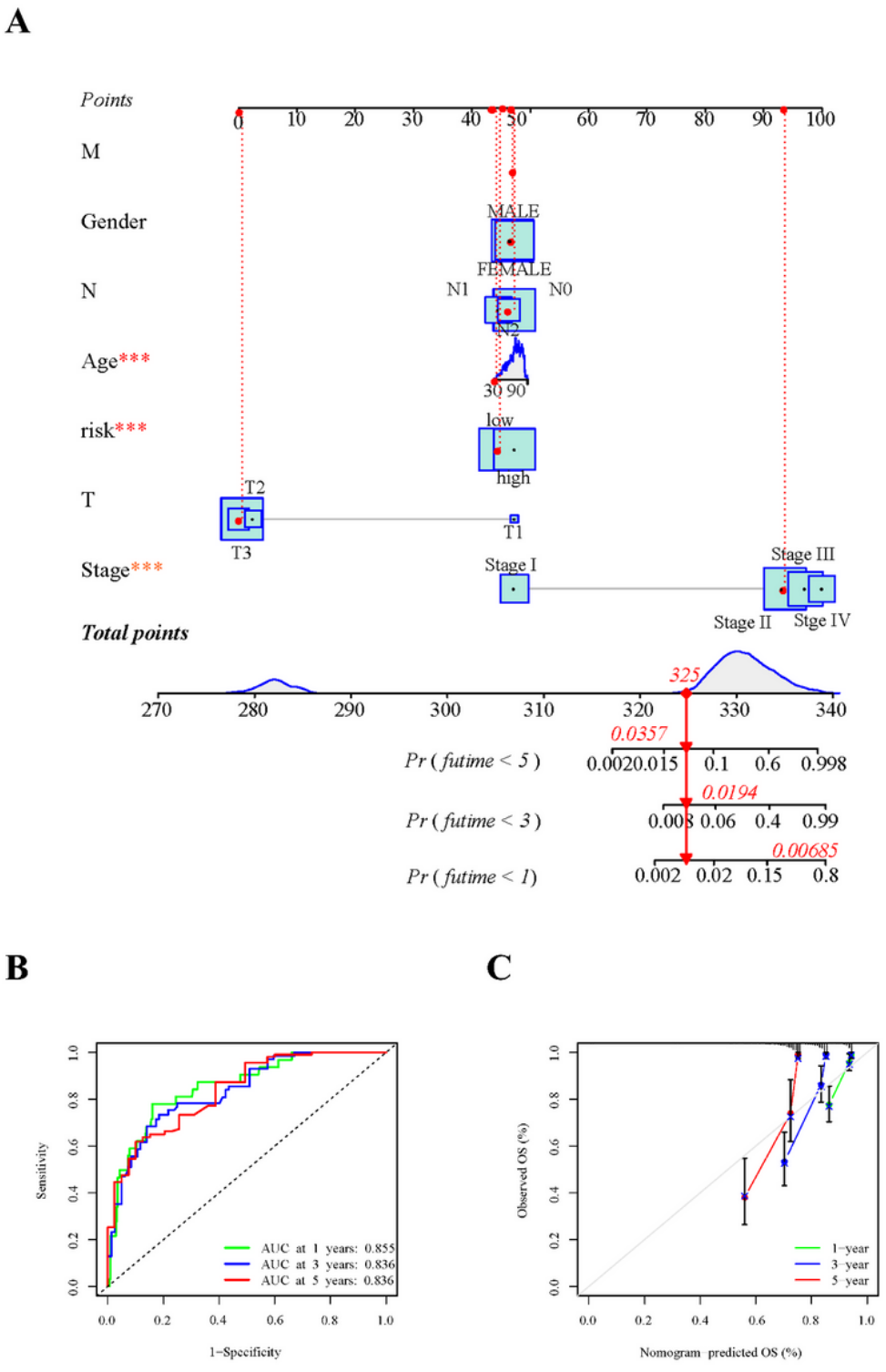

Figure 3

Nomogram. (A) Nomogram that could predict the prognosis of patients with COAD. (B) ROC curve of the nomogram for 1 year, 3 years, and 5 years. (C) Calibration curve of the ROC curve of the nomogram for 1 year, 3 years, and 5 years.

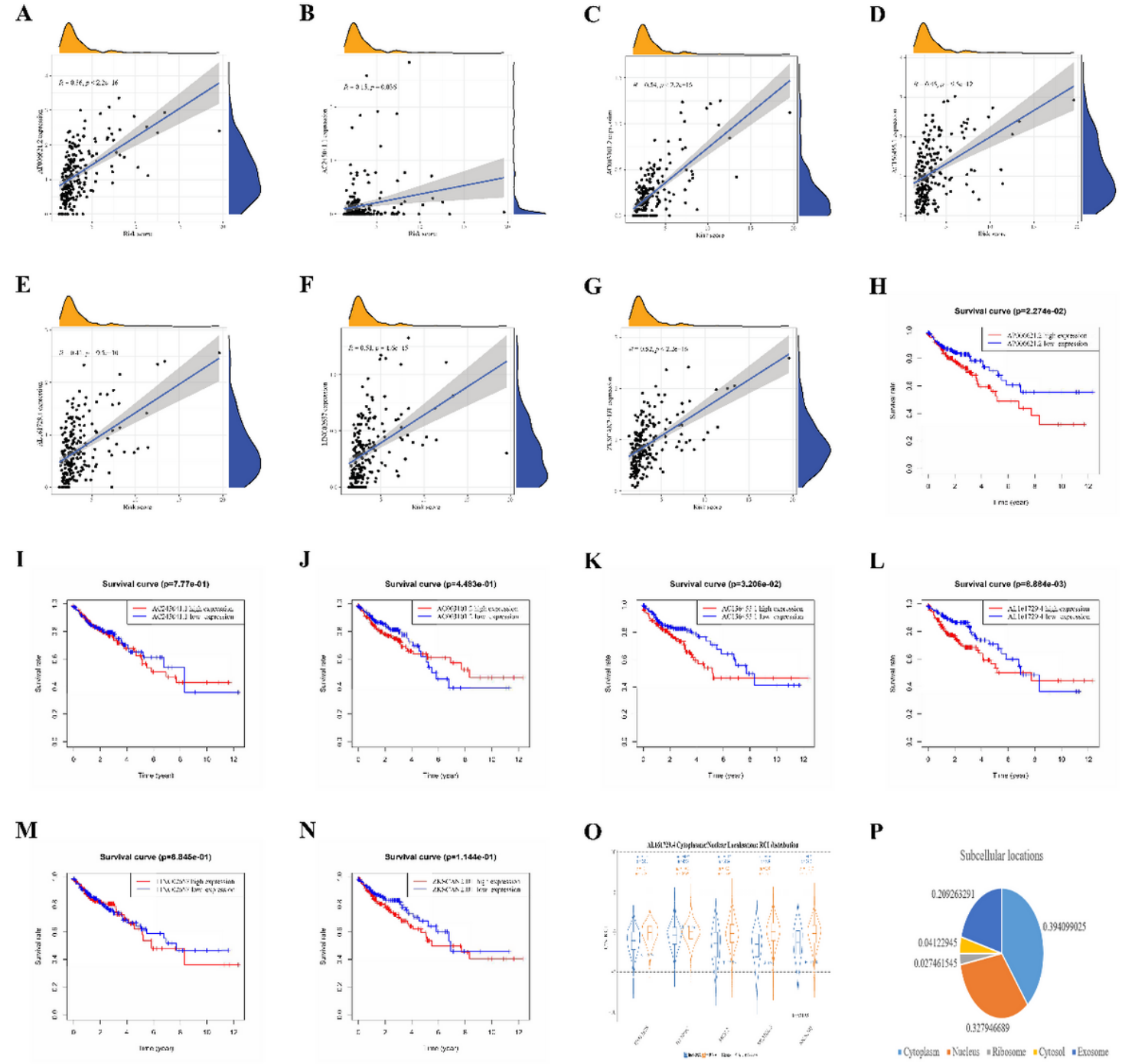

Figure 4

Functional analysis of the prognostic risk model lncRNA. (A-G) Relationship between AC003101.2, LINC02657, L161729.4, AP006621.2, AC156455.1, ZKSCAN2-DT, and AC245041.1 and the risk score. (H-N) Survival difference between the high-expression and low-expression groups of AC003101.2, LINC02657, AL161729.4, AP006621.2, AC156455.1, ZKSCAN2-DT, and AC245041.1. (O) Subcellular

localization of AL161729.4 in GM12878, H1-hESC, MCF-7, SK-MEL-5, and SK-N-SH cells. (P) Subcellular localization of AL161729.4.

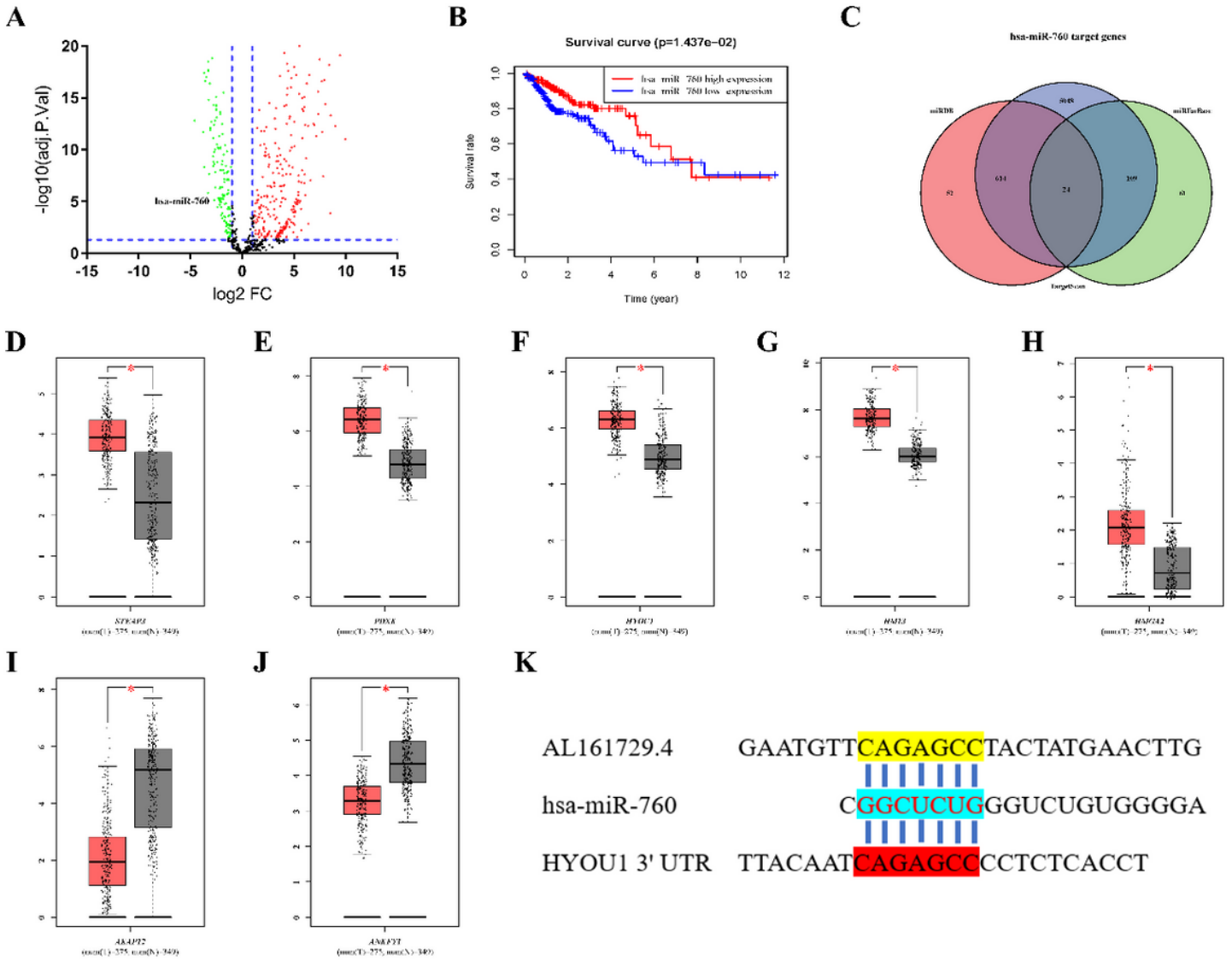

Figure 5

Construction of the ceRNA network. (A) MiRNAs that are differentially expressed between patients with COAD and normal samples. (B) A significant difference in survival was found between the miR-760 high-expression and low-expression groups. (C) Target genes of miR-760 in miRDB, miRTarBase, and TargetScan databases. (D-J) Expression differences of STEAP3, PDXK, HYOU1, HMGA2, AKAP12, and ANKFY1 between patients with COAD and normal samples. (K) Base complementation between AL161729.4-miR-760-HYOU1.

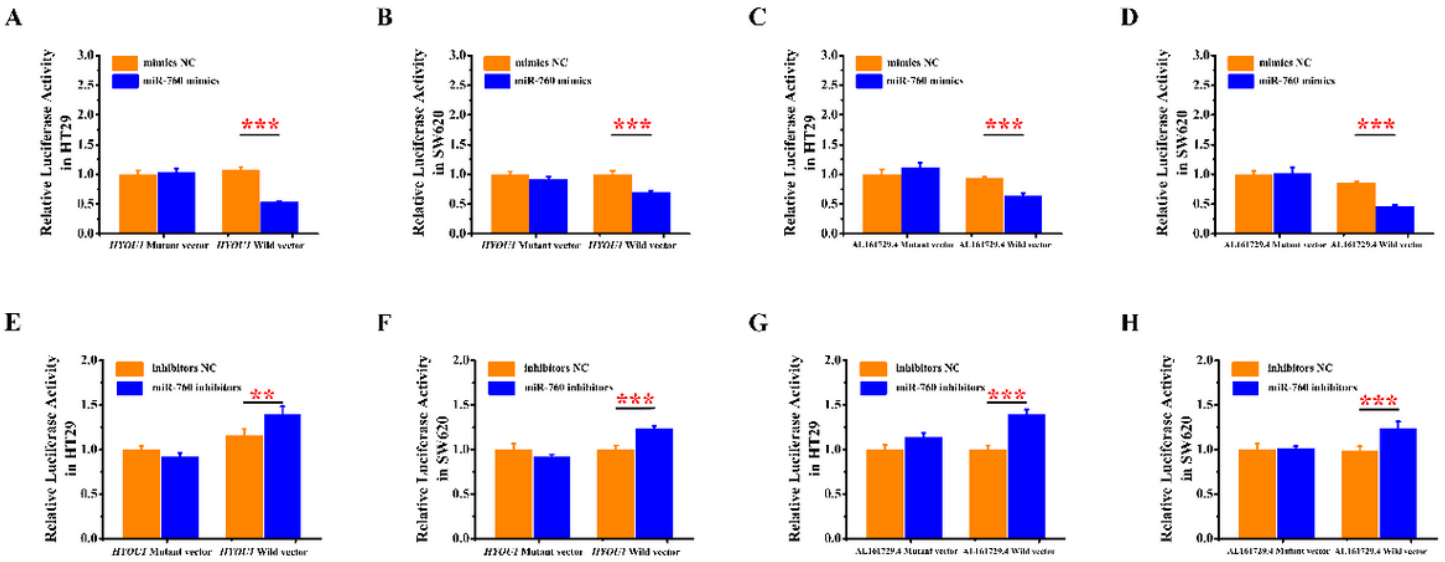

Figure 6

Verification of ceRNA network. (A) miR-760 mimics could reduce the fluorescence level of the HYOU1 wild-type vector in HT29 cells. (B) miR-760 mimics could reduce the fluorescence level of the HYOU1 wild-type vector in SW620 cells. (C) miR-760 mimics could reduce the fluorescence level of the AL161729.4 wild-type vector in HT29 cells. (D) miR-760 mimics could reduce the fluorescence level of the AL161729.4 wild-type vector in SW620 cells. (E) miR-760 inhibitors could increase the fluorescence level of the HYOU1 wild-type vector in HT29 cells. (F) miR-760 inhibitors could increase the fluorescence level of the HYOU1 wild-type vector in SW620 cells. (G) miR-760 inhibitors could increase the fluorescence level of the AL161729.4 wild-type vector in HT29 cells. (H) miR-760 inhibitors could increase the fluorescence level of the AL161729.4 wild-type vector in SW620 cells.

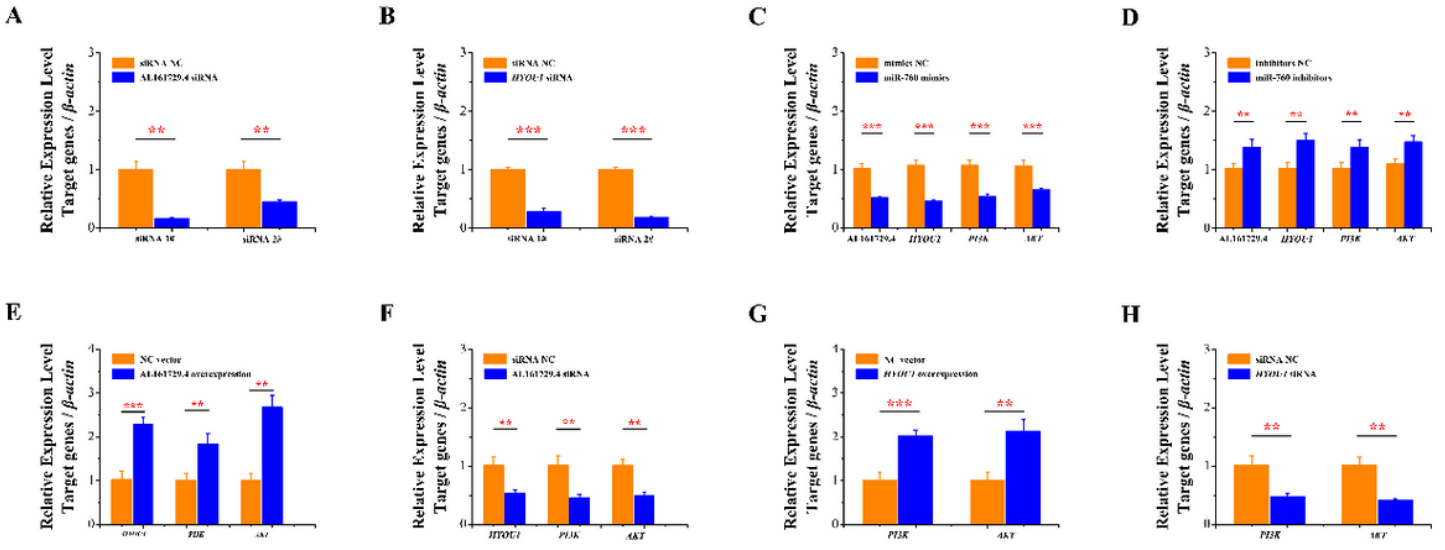

Figure 7

AL161729.4-miR-760-HYOU1 was involved in the regulation of the PI3K/Akt signaling pathway. (A) Comparison of knockdown effects of AL161729.4 siRNA 1# and siRNA 2#. (B) Comparison of knockdown effects of HYOU1 siRNA 1# and siRNA 2#. (C) miR-760 mimics could significantly reduce the mRNA levels of AL161729.4, HYOU1, PI3K, and Akt. (D) miR-760 inhibitors could significantly increase the mRNA levels of AL161729.4, HYOU1, PI3K, and Akt. (E) Overexpression of AL161729.4 could significantly increase the mRNA levels of HYOU1, PI3K, and Akt. (F) Knockdown of AL161729.4 could significantly reduce the mRNA levels of HYOU1, PI3K, and Akt. (G) Overexpression of HYOU1 could significantly increase the mRNA levels of PI3K and Akt. (H) Knockdown of HYOU1 could significantly reduce the mRNA levels of PI3K and Akt.

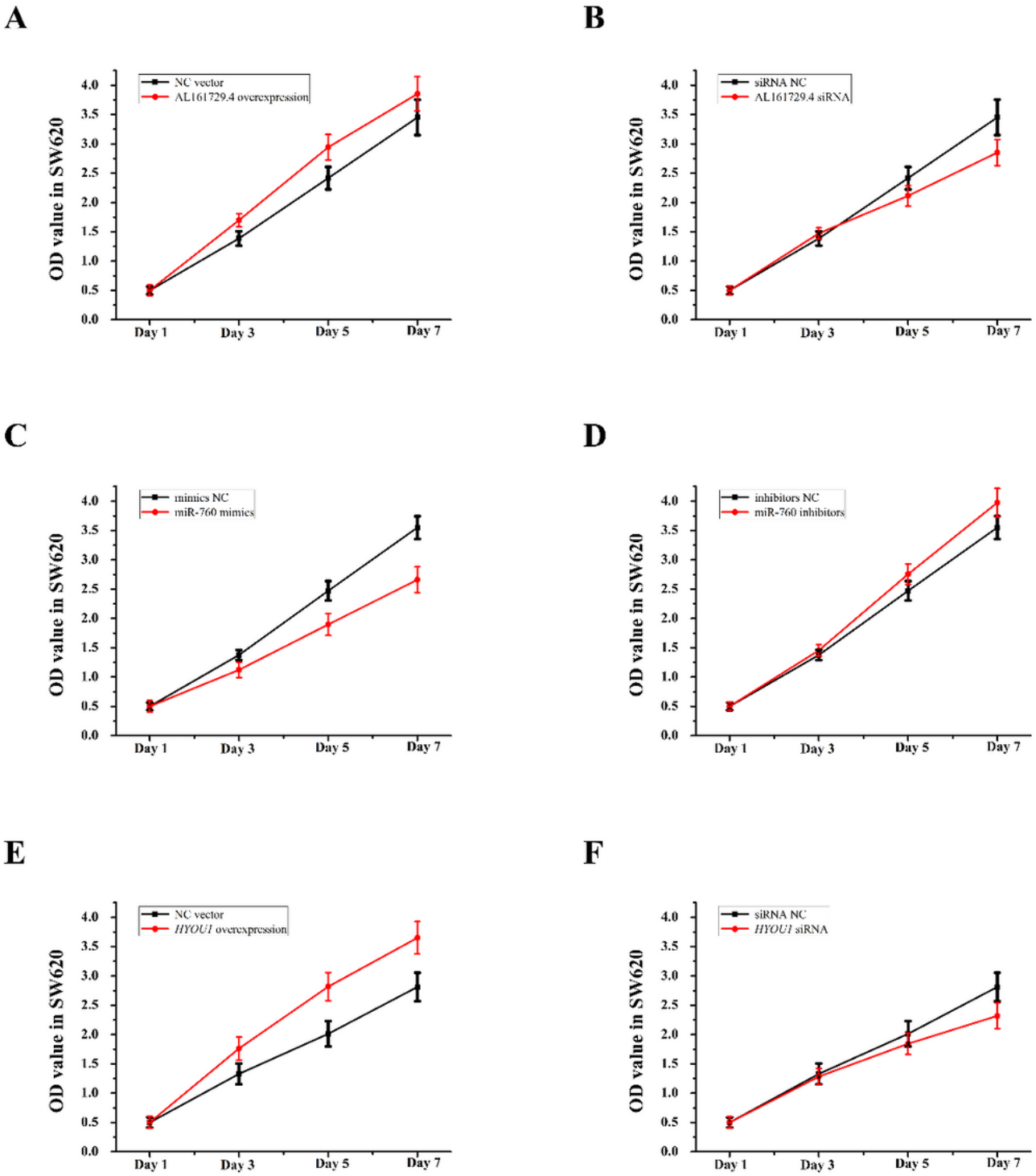

Figure 8

AL161729.4-miR-760-HYOU1 was involved in the proliferation of SW620 cells. (A) Overexpression of AL161729.4 could promote the proliferation of SW620 cells. (B) Knockdown of AL161729.4 could reduce the proliferation of SW620 cells. (C) miR-760 mimics could reduce the proliferation of SW620 cells. (D) miR-760 inhibitors could promote the proliferation of SW620 cells. (E) Overexpression of HYOU1 could

promote the proliferation of SW620 cells. (F) Knockdown of HYOU1 could reduce the proliferation of SW620 cells.